

Signatures of homoclinic motion in quantum chaos

D. A. Wisniacki,^{1,2} E. Vergini,^{1,3} R. M. Benito,⁴ and F. Borondo^{1,*}

¹*Departamento de Química C-IX, Universidad Autónoma de Madrid, Cantoblanco, 28049-Madrid, Spain.*

²*Departamento de Física “J. J. Giambiagi”, FCEN, UBA, 1428 Buenos Aires, Argentina.*

³*Departamento de Física, Comisión Nacional de Energía Atómica. Av. del Libertador 8250, 1429 Buenos Aires, Argentina.*

⁴*Departamento de Física, E.T.S.I. Agrónomos, Universidad Politécnica de Madrid, 28040 Madrid, Spain.*

(Dated: November 13, 2018)

Homoclinic motion plays a key role in the organization of classical chaos in Hamiltonian systems. In this Letter, we show that it also imprints a clear signature in the corresponding quantum spectra. By numerically studying the fluctuations of the widths of wavefunctions localized along periodic orbits we reveal the existence of an oscillatory behavior, that is explained solely in terms of the primary homoclinic motion. Furthermore, our results indicate that it survives the semiclassical limit.

PACS numbers: 05.45.Mt, 03.65.Sq

Periodic orbits (POs) are invariant classical objects of outmost relevance for the understanding of chaotic dynamical systems. The pioneering work of Poincaré demonstrated the importance of these retracing orbits in organizing the complexity of the corresponding classical motion. Semiclassically, Gutzwiller [1] developed his celebrated trace formula, able to quantize chaotic systems, solely in terms of POs information. Quantum mechanically, striking manifestations of POs have been reported in the literature. One of the most important are “scars” [2], an enhanced localization of quantum density along unstable short POs in certain individual eigenfunctions. This phenomenon was first noticed in the Bunimovich stadium billiard [3], and subsequently studied systematically by Heller, who constructed a theory of scarring based on wave packet propagation [4]. Another important contribution to scar theory is due to Bogomolny [5], who derived an explicit expression for the PO contributions to the smoothed quantum probability density over small ranges of space and energy (i.e. average over a large number of eigenfunctions). A corresponding theory for Wigner functions was developed by Berry [6]. Recently, there has been a flurry of activity focusing on the influence of bifurcations (mixed systems) on scarring [7].

The existence of a scar implies a clear regularity in the corresponding quantum spectrum, related to the period of the PO. In time domain, the dynamics of a packet running along a PO induce recurrences in the autocorrelation function, that when Fourier transformed define an envelope in the spectrum, giving rise to peaks of width proportional to the Lyapunov exponent, λ , at energies given by a Bohr–Sommerfeld (BS) quantization condition [1, 8].

In this Letter, we demonstrate the existence of an additional superimposed spectral regularity also related to scarring. It is originated by the associated homoclinic motion and is given by the area enclosed by the stable and unstable manifolds up to the first crossing. To unveil this regularity we consider the fluctuations of the

spectral widths corresponding to localized wavefunctions along unstable POs. Our data demonstrate that these fluctuations have a surprisingly simple oscillatory behavior essentially governed by the quantization of only the primary homoclinic dynamics. We provide an explanation of this result in terms of the coherence of this classical motion [9], which constitute the natural global extension of the local hyperbolic structure around the PO. Furthermore, our numerical results indicate that the observed oscillatory behavior do not vanish as $\hbar \rightarrow 0$.

It should be remarked that, contrary to the previously described results on scar theory, our study implies dynamics beyond the Ehrenfest time ($\sim |\ln \hbar|$), when the PO manifolds start to cross and the homoclinic tangle develops, giving rise to subtle quantum interference effects. Other interesting papers, also considering these longer times, are due to Tomsovic and Heller [10], who showed how to construct a valid semiclassical approximation to wavefunctions past this limit; this came as a surprise since the underlying chaos has had time to develop much finer structure than a quantum cell. Similarly to what happens in energy domain with Gutzwiller trace formula, this theory unfortunately requires the use of a number of homoclinic excursions increasing exponentially with time. Our result indicates that there exists some properties of these long term dynamics that can be understood in terms of a small number of classical invariants.

The ideal tool to carry out our investigation are non-stationary wave functions highly localized on POs. The overlap with the corresponding eigenstates provides information on how these structures appear in the spectra, and how they are embedded in the quantum mechanics of the system. Such functions, associated to a PO, can be obtained by using the (dynamical) information up to the Ehrenfest time, thus including the hyperbolic structure formed by the corresponding unstable and stable manifolds. In this way, the associated wavefunctions spread along these dynamically relevant regions of phase space (see illustration below in Fig. 1). This can be done in

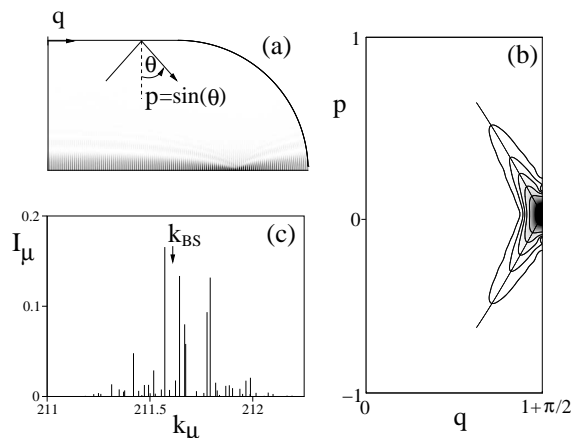


FIG. 1: Configuration space (a), phase space (b), and wavelength spectrum weights (c) representations of a scar wavefunction along the horizontal periodic orbit of a desymmetrized stadium billiard corresponding to BS wavelength $k_{BS} = 211.665$. The unstable and stable manifolds of the orbit are also plotted in panel (b). In panel (a) the Birkhoff coordinates on the boundary of the billiard are shown.

different ways [11, 12]; in particular, in Ref. 12 a definition of scar functions, based on transversally excited resonances along POs at given BS quantized energies with minimum dispersion, is provided. The width of these functions in the energy spectrum is given by,

$$\sigma_{sc} = \frac{\pi\hbar\lambda}{|\ln\hbar|} + \mathcal{O}\left(\frac{\hbar}{|\ln\hbar|^2}\right), \quad (1)$$

where the narrowing factor $|\ln\hbar|^{-1}$ comes from the inclusion of the hyperbolic structure [12]. In this respect, it should be noticed that although this approach incorporates the motion along the manifolds up to the Ehrenfest time, interference effects due to the intersections of the manifolds are not included.

The model used in our calculations is the fully chaotic system consisting of a particle of mass M confined in a desymmetrized Bunimovitch stadium billiard, defined by the radius of the circular part, $r = 1$, and the enclosed area, $1 + \pi/4$. To calculate the corresponding eigenstates, Dirichlet conditions on the stadium boundary and Neumann conditions on the symmetry axes are imposed. We will focus our attention on the dynamics influenced by the horizontal PO. The corresponding scar wavefunctions, $|\gamma\rangle$, are calculated using the method of Ref. [12].

In Fig. 1 we show, as an example, the results for the scar state with wavelength $k_{BS} = 211.665$. This value was obtained from the BS rule, $k_{BS} = (2\pi/L_H)(n + \nu_H/4)$, where $n = 134$ is the excitation number along the orbit, $L_H = 4$ its length, and $\nu_H = 3$ the corresponding Maslov index. In it, all features discussed above are observed. Namely, the Husimi based quantum surface of section [13] spreads along the manifolds

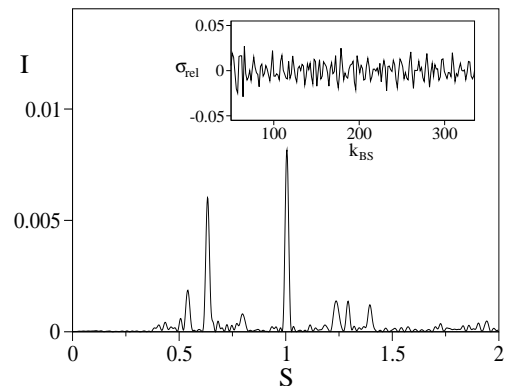


FIG. 2: Relative width for the scar states along the horizontal periodic orbit as a function of the Bohr-Sommerfeld quantized wavelength (inset), and its Fourier transform.

structure associated to the horizontal PO, and the state appears in the spectrum distributed among the different eigenstates, $|\mu\rangle$, within a given range around the corresponding BS quantized wavelength, with intensity weights $I_\mu \equiv |\langle\mu|\gamma\rangle|^2$.

The energy width of the associated envelope can then be defined as (we take $M = \hbar^2/2$ in such a way that k^2 is the energy of the particle)

$$\sigma = \sqrt{\sum_{\mu} |\langle\mu|\gamma\rangle|^2 (k_{\mu}^2 - k_{BS}^2)^2}. \quad (2)$$

When calculated, this quantity is a decreasing oscillatory function of k_{BS} , that can be more adequately studied by defining its relative variation with respect to the corresponding semiclassical value,

$$\sigma_{rel} \equiv \frac{\sigma - \sigma_{sc}}{\sigma_{sc}}. \quad (3)$$

The corresponding results are shown in the inset to Fig. 2. As can be observed, it exhibit an oscillatory behavior, with an amplitude representing only a small fraction of σ_{sc} . When this signal is Fourier analyzed (see main body of Fig. 2) it is seen to have only two relevant components, corresponding to the peaks appearing at values of the action $S = 0.633$ and 1.007 , respectively. (Notice that, in our case, S has units of length since the total linear momentum of the particle has been set equal to one). The BS quantization of the wavelength implies that the Fourier transform of σ_{rel} is a periodic function with period L_H . In this respect, corresponding peaks appear at $S = -3.367$ and -2.993 .

To interpret this result, we consider only the primary homoclinic motion corresponding to the horizontal PO. This follows the analysis of Ozorio de Almeida [9], who studied the quantization of homoclinic orbits, that were thought of as defining an invariant torus, approached by series of satellite unstable POs. There are two topologically distinct types of primary homoclinic points, which

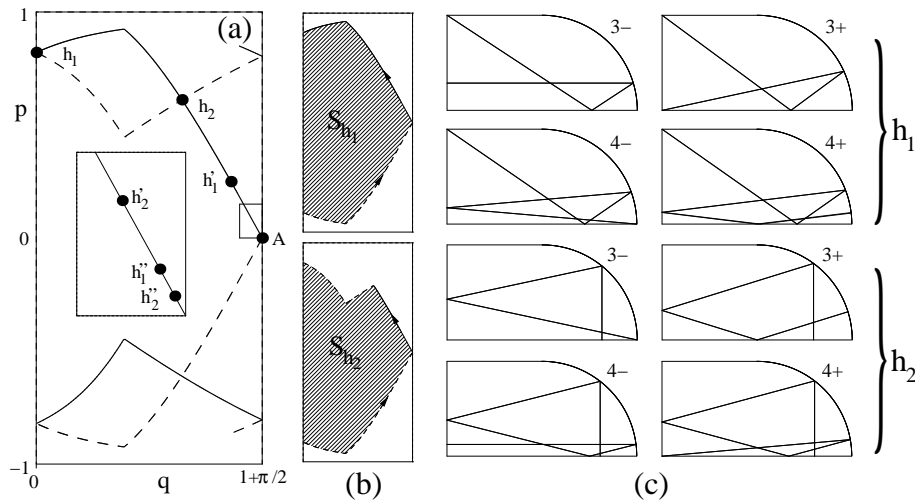


FIG. 3: (a) Phase space portrait in Birkhoff coordinates relevant to our calculations. Label A indicates the position of the fixed point corresponding to the horizontal periodic orbit. The associated unstable and stable manifolds are represented in full and dashed line, respectively. They cross, with different topology, at the primary homoclinic points h_1 and h_2 , which map into $h_1', \dots, h_1'', \dots$, and h_2', h_2'', \dots . (b) Primary homoclinic areas S_{h_1} and S_{h_2} associated to the horizontal orbit. (c) Satellite periodic orbits converging to the homoclinic points h_1 and h_2 . See text for details.

appear as the first and second intersections of the associated manifolds. The situation is shown in Fig. 3 (a), where a picture of the relevant phase space, in Birkhoff coordinates, is presented. In it, we have plotted the fixed point corresponding to the horizontal PO (labelled A), and the emanating unstable (full line) and stable (dashed line) manifolds. These manifolds first cross (with different topology) at points h_1 and h_2 , and afterwards at the sequences h_1', h_1'', \dots , and h_2', h_2'', \dots (and their reflections with respect to $p = 0$), as fixed point A is approached. These infinite sequences of points, which are the dynamical images of h_1 and h_2 , constitute the primary homoclinic orbits, that define two relevant areas in phase space, denoted hereafter as S_{h_1} and S_{h_2} [see shaded regions in Fig. 3 (b)], important for the discussions presented below. Furthermore, these primary homoclinic orbits accumulate infinite sets of satellite POs with increasingly longer periods, as discussed in Ref. [14]. The first members of these two families, converging to the primary homoclinic orbits are presented in Fig. 3 (c). Accordingly to our notation, based on the number of times that the POs intersect our surface of section, orbits 3- and 3+ consist of fixed points near h_1, h_1' (or h_2, h_2'), and their reflections with respect to $p = 0$; orbits 4- and 4+ consists of fixed points near h_1, h_1', h_1'' (or h_2, h_2', h_2''), and their reflections; and so on for the longer POs in the family. Notice that the reflection with respect to $p = 0$ of points over $q = 0$ or $q = 1 + \pi/2$ gives the same point. Moreover, these POs can be grouped in pairs, in such a way that 3- and 3+ represent the first approximation to the primary homoclinic motion (the - indicates the PO with shortest length of the pair), 4- and 4+ the second,

etc. Actually, it is apparent the increasing relation of these orbits to the horizontal one, since as we progress in the sequence new segments closer and closer to the horizontal axis are incorporated into the trajectory.

Now, the question arises about under which conditions the satellite families of POs reinforce the contribution of the central one. As seen before, the horizontal PO satisfy the BS quantization condition

$$kL_H - \frac{\pi}{2}\nu_H = 2\pi n_H, \quad (4)$$

being n_H an integer. In the same way, the BS condition for orbits crossing m times the surface of section reads

$$kL_m - \frac{\pi}{2}\nu_m = 2\pi n_m. \quad (5)$$

Subtracting m times Eq. (4) to (5), a new quantization condition emerges

$$k(L_m - mL_H) - \frac{\pi}{2}(\nu_m - m\nu_H) = 2\pi(n_m - mn_H). \quad (6)$$

The relevant point here is that $L_m - mL_H$ converges exponentially to $S_{h_1} = -3.368\ 390\ 45$ and $S_{h_2} = -2.991\ 142\ 22$ for the two families h_1 and h_2 , respectively, as shown in Table I. Moreover, $\nu_m - m\nu_H$ is independent of m , and it corresponds to $\nu_{h_1} = -1$ and $\nu_{h_2} = 0$. In this way, we are in the position to assess that all satellite orbits of a given family contribute coherently when two BS quantization rules are simultaneously fulfilled: (a) the quantization of the central (horizontal) orbit [Eq. (4)], and (b) the so-called quantization of the homoclinic torus according to Ref. [9],

$$kS_{h_i} - \frac{\pi}{2}\nu_{h_i} = 2\pi n, \quad i = 1, 2. \quad (7)$$

m	$\bar{L}_m - mL_H$	
	Family h_1	Family h_2
3	-3.367 727 48	-2.990 915 39
4	-3.368 367 57	-2.991 131 87
5	-3.368 389 68	-2.991 141 81
6	-3.368 390 43	-2.991 142 21
7	-3.368 390 45	-2.991 142 22

TABLE I: Exponential convergence of $\bar{L}_m - mL_H$ as a function of the number of times the POs intersect our surface of section for families h_1 and h_2 of satellite orbits corresponding to the primary homoclinic motion. To improve the convergence we have averaged the length of orbits $m+$ and $m-$ for the same family [see Fig. 3 (c)].

It should be observed that the values of S_{h_1} and S_{h_2} agree extremely well with those obtained numerically for the position of the two main peaks in the spectrum of Fig. 2. On the other hand, these homoclinic areas correspond in our chosen Poincaré surface of section to the areas indicated in Fig. 3 (b). The arrows in Fig. 3 (b) indicate the anti-clockwise direction of the homoclinic motion, and for this reason homoclinic areas result negative.

This notorious influence of the homoclinic motion in the spectra, and thus in the quantum mechanics of our system, is remarkable, especially, when one takes into account that the homoclinic dynamics is the origin of the chaotic behavior in Hamiltonian systems. In order to understand this behavior we note that the motion has two components. The first one, close to the primary homoclinic torus, is such that the corresponding trajectories interfere coherently, as it has been shown. The second component, associated to the non-primary homoclinic crosses, gives rise to more complicated self-intersecting tori. These excursions are much longer and the corresponding interference is much less coherent; accordingly, its influence in the spectra is very diluted. In this respect, it is more efficient to consider these long excursions, by the interaction with other short POs (heteroclinic connections). This point has been discussed elsewhere [15].

Finally, let us consider if the influence of the homoclinic motion on σ_{rel} survives the semiclassical limit $\hbar \rightarrow 0$ ($k = \frac{1}{\hbar} \rightarrow \infty$ in our units). For this purpose we have performed the following calculation. Starting from the scaled fluctuation curve σ_{rel} , presented in the inset to Fig. 2, we compute the Fourier transform of the function for increasingly larger intervals of k_{BS} , (k_0, k_1), keeping fixed the value of the lower limit, k_0 . The results for the peak at S_{h_1} are shown in Fig. 4, where it is seen that the corresponding Fourier intensity divided by $(\Delta k)^2$ is an approximately constant function of the length of the interval, $\Delta k = k_1 - k_0$. A similar behavior is obtained for the peak at S_{h_2} . This result implies that $\sigma_{\text{rel}}(k_{\text{BS}})$

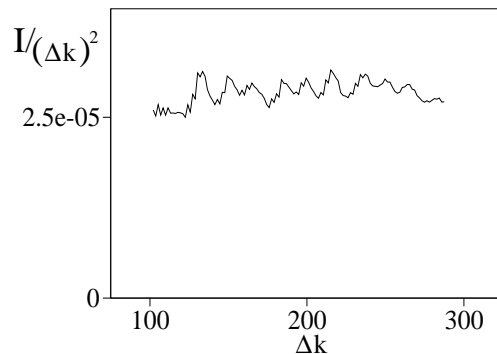


FIG. 4: Intensity of the peak at S_{h_1} divided by $(\Delta k)^2$ as a function of Δk

is essentially an oscillatory function with frequencies S_{h_1} and S_{h_2} and constant coefficients.

In conclusion, we have gone one step further the usual understanding of the quantum–classical correspondence, by showing how homoclinic areas imprint a clear signature in the spectra of classically chaotic systems. In particular, we have found that the fluctuations of the relative widths corresponding to wavefunctions (with hyperbolic structure) highly localized in the vicinity of a PO oscillate in a very simple way, that is clearly controlled by the quantization of the associated primary homoclinic motions. This indicates the importance of classical invariants, other than those included in Gutzwiller theory concerning individual POs, for the systematic description of quantum information.

This work was supported by MCyT and MCEd (Spain) under contracts BQU2003–8212, SAB2000–340, and SAB2002–22.

* E–mail address: f.borondo@uam.es

- [1] M. C. Gutzwiller, *Chaos in Classical and Quantum Mechanics* (Springer–Verlag, New York, 1990).
- [2] E. J. Heller, Phys. Rev. Lett. **53**, 1515 (1984).
- [3] S. W. McDonald, *LBL Report* 14837 (1983).
- [4] L. Kaplan and E. J. Heller, Ann. Phys. **264**, 171 (1998).
- [5] E. B. Bogomolny, Physica D **31**, 169 (1988).
- [6] M. V. Berry, Proc. R. Soc. Lon. A **243**, 219 (1989).
- [7] J. P. Keating and S. D. Prado, Proc. R. Soc. Lon. A **457**, 1855 (2001).
- [8] E. J. Heller, in *Chaos and Quantum Physics*, edited by M. J. Giannoni, A. Voros, and J. Zinn–Justin (Elsevier, Amsterdam, 1991).
- [9] A. M. Ozorio de Almeida, Nonlinearity **2**, 519 (1989).
- [10] S. Tomsovic and E. J. Heller, Phys. Rev. Lett. **70**, 1405 (1993); Phys. Rev. E. **47**, 282 (1993).
- [11] G. G. de Polavieja, F. Borondo, and R. M. Benito, Phys. Rev. Lett. **73**, 1613 (1994).
- [12] E. G. Vergini and G. Carlo, J. Phys. A **34**, 4525 (2001).
- [13] D. A. Wisniacki, F. Borondo, E. Vergini, and R. M. Ben-

- ito, Phys. Rev. E **63**, 66220 (2001).
- [14] G. L. Da Silva Ritter, A. M. Ozorio de Almeida, and R. Douady, Physica D **29**, 181 (1987).
- [15] D. A. Wisniacki, F. Borondo, E. Vergini, and R. M. Benito, Phys. Rev. E **70**, 035202(R) (2004).